J Neurophysiol 102: 2982–2993, 2009.
First published September 9, 2009; doi:10.1152/jn.00545.2009.

Direct Activation and Temporal Response Properties of Rabbit Retinal Ganglion Cells Following Subretinal Stimulation

David Tsai,[1] John W. Morley,[2,3] Gregg J. Suaning,[1] and Nigel H. Lovell[1]

[1]*Graduate School of Biomedical Engineering and* [2]*School of Medical Sciences, University of New South Wales; and* [3]*School of Medicine, University of Western Sydney, Sydney, New South Wales, Australia*

Submitted 22 June 2009; accepted in final form 7 September 2009

Tsai D, Morley JW, Suaning GJ, Lovell NH. Direct activation and temporal response properties of rabbit retinal ganglion cells following subretinal stimulation. *J Neurophysiol* 102: 2982–2993, 2009. First published September 9, 2009; doi:10.1152/jn.00545.2009. In the last decade several groups have been developing vision prostheses to restore visual perception to the profoundly blind. Despite some promising results from human trials, further understanding of the neural mechanisms involved is crucial for improving the efficacy of these devices. One of the techniques involves placing stimulating electrodes in the subretinal space between the photoreceptor layer and the pigment epithelium to evoke neural responses in the degenerative retina. This study used cell-attached and whole cell current-clamp recordings to investigate the responses of rabbit retinal ganglion cells (RGCs) following subretinal stimulation with 25-μm-diameter electrodes. We found that direct RGC responses with short latency ($\leq$2 ms using 0.1-ms pulses) could be reliably elicited. The thresholds for these responses were reported for ON, OFF, and ON–OFF RGCs over pulse widths 0.1–5.0 ms. During repetitive stimulation these direct activation responses were more readily elicited than responses arising from stimulation of the retinal network. The temporal spiking characteristics of RGCs were characterized as a function of stimulus configurations. We found that the response profiles could be generalized into four classes with distinctive properties. Our results suggest that for subretinal vision prostheses short pulses are preferable for efficacy and safety considerations, and that direct activation of RGCs will be necessary for reliable activation during high-frequency stimulation.

INTRODUCTION

Retinal degenerative diseases such as retinitis pigmentosa and age-related macular degeneration are currently the leading cause of blindness in developed countries (Klaver et al. 1998). As the population ages, it is expected that the prevalence of these diseases will increase significantly in the years to come (Friedman et al. 2004). Several research groups are actively developing strategies to restore vision in profoundly blind individuals through electrical stimulation of the retina (Fujikado et al. 2007; Gerding et al. 2002; Humayun et al. 1999; Völker et al. 2004; Wong et al. 2009; Zhou et al. 2008) and trials on blind subjects have shown that simple percepts, such as bright spots, could be generated (Fujikado et al. 2007; Gekeler et al. 2006; Humayun et al. 2003; Rizzo et al. 2003a). Although promising, the elicited percepts were rudimentary and, in many cases, also unexpected (Rizzo et al. 2003). Our ability to improve the efficacy of these prosthetic devices will depend critically on further understanding of the retinal neural mechanisms involved during electrical activation and how these mechanisms may be controlled artificially to produce clinically useful vision.

Stimulating electrodes may be placed at any one of the several locations relative to the retina. The subretinal approach involves placing the electrodes between the photoreceptor layer and retinal pigment epithelium. Several authors have previously studied the effect of subretinal stimulation on retinal ganglion cells (RGCs) using a variety of animal models (Jensen and Rizzo 3rd 2006, 2007, 2008; Li et al. 2005; O'Hearn et al. 2006; Shyu et al. 2006; Stett et al. 2000). With the exception of Stett et al. (2000), Li et al. (2005), and Jensen and Rizzo 3rd (2008), existing subretinal studies have primarily focused on the thresholds for eliciting neural responses. It has been observed previously (Li et al. 2005; Stett et al. 2000) that the temporal response profiles of RGCs following subretinal stimulation were diverse and varied with stimulus configuration. Thus the question arises whether there exist patterns in the RGC response profile and, if so, how these patterns relate to the stimulus configurations. Furthermore, studies using epiretinal stimulations, in which the electrodes were placed adjacent to the RGC layer, have shown that short-latency stimulus-locked RGC spikes could be reliably elicited (Fried et al. 2006; Sekirnjak et al. 2006). Such responses have not been conclusively demonstrated for the subretinal approach.

Here we studied the responses of RGCs following subretinal stimulation using cell-attached and whole cell current-clamp recordings in the rabbit retina. We began by demonstrating that subretinal stimulation with small electrodes (25-μm diameter) can reliably elicit short-latency direct RGC spikes. The robustness of these direct responses during repetitive stimulation was examined at a range of frequencies and pulse widths. We also quantitatively investigated the temporal response profiles of RGCs following electrical stimulation, as a function of stimulus amplitude and duration.

METHODS

Retinal whole-mount preparation

All procedures were reviewed and approved by the UNSW Animal Care and Ethics Committee. New Zealand White rabbits (2–3.5 kg) were anesthetized with an intramuscular injection of ketamine (70 mg/kg) and xylazine (10 mg/ml) and supplemented intravenously as needed. An eye was enucleated. The animal was then killed by sodium pentobarbital overdose. The eye was hemisected 2–3 mm behind the ora serrata. The front portion of the eye and the vitreous were discarded. Three pieces of the inferior retina inclusive of the visual streak were dissected free with the underlying sclera and placed in an incubation chamber containing Ames' medium (Sigma–Aldrich) with

Address for reprint requests and other correspondence: N. H. Lovell, Graduate School of Biomedical Engineering, University of New South Wales, Sydney, NSW 2125, Australia (E-mail: N.Lovell@unsw.edu.au).

1% penicillin/streptomycin (Invitrogen) equilibrated to pH 7.4 at either 25 or 31°C for 1 h before being transferred to a room temperature holding chamber and kept for ≤10 h before recording.

To assist visualization, prior to recording the RGCs were labeled by immersing a piece of the retina, with the attached sclera, in Ames' medium containing 1 mg/ml of Azure B (Sigma–Aldrich) (Amthor et al. 2002; Hu et al. 2000) for 45 s. The neural retina was then separated from the pigment epithelium and mounted photoreceptor side up in an imaging chamber on an inverted microscope with poly-L-lysine (Sigma–Aldrich) at 1 mg/ml. The retinas were perfused with Ames' medium at 5 ml/min, equilibrated with 95% O_2-5% CO_2 to pH 7.4 and heated to 34–35°C.

Light stimulation

A stationary spot of light emitted by a white LED behind a pinhole was projected onto the retina via the ×10 objective of the microscope. The spot was centered over the soma of the targeted RGC and had a diameter of 250 μm when focused on the photoreceptor layer.

To determine the light response type of the recorded cell, a 4-s alternating sequence consisting of ON–OFF–ON–OFF, each of 1 s, was presented. This was repeated five times with 5 s between each presentation. The entire process was then repeated for the alternating sequence OFF–ON–OFF–ON.

Cells were considered transient if their responses returned to baseline by the end of the 1-s light stimulus; otherwise, they were considered sustained (Roska and Werblin 2001).

Electrical stimulation

Constant-current charge-balanced biphasic stimuli were generated by a custom-made neural stimulator capable of delivering ≤200 μA of current. The stimulation electrodes were fabricated from a platinum–iridium (Pt-Ir) wire (A-M Systems) of 25-μm diameter coated with Teflon, with only the transversely cut circular tip exposed. Electrodes were placed at the photoreceptor side under visual guidance to a lateral distance of 55 ± 10 μm from the soma of the target cell (Fig. 1*A*) to avoid mechanical disturbance of the patched cell during positioning. The stimulation return electrode consisted of a distant platinum wire loop in the perfusion bath about 2 cm away from the stimulation electrode (monopolar configuration). All biphasic pulses were cathodic-first, followed immediately by the anodic component without interpulse delay.

In this study we defined the stimulation threshold to be the current required to elicit RGC action potential(s) in ≥10 of 20 consecutive trials (50%) with a 1-s delay between trials to minimize potential long-duration effects of repetitive stimulation (Jensen and Rizzo 3rd 2008). Response latencies were measured from the onset of the stimulus artifact to the peak of the action potentials.

For repetitive stimulation with pulse trains, the stimulus amplitudes were set at 110 ± 10% of the cell's threshold (as defined earlier) at the given pulse duration. Each pulse train consisted of four identical biphasic pulses. The repetition frequencies attempted were (Hz): 50, 66.7, 100, and 200. At each frequency three pulse widths were tested (ms): 0.1, 0.2, and 0.5. For each frequency and pulse-width configuration pair, the stimulus train was repeated 20 times, with a 1-s delay between repeats.

Recording of retinal ganglion cell responses

RGC responses were recorded with either cell-attached recording or whole cell current clamp (I_h = 0 nA) using a Multiclamp 700B amplifier (Molecular Devices). Data were low-pass filtered at 3 kHz and digitized at 10 kHz with a Digidata 1440A and pCLAMP 10 software (Molecular Devices). All recordings were carried out under mesopic lighting. The retinas were visualized with either Hoffman Modulation Contrast or Nomarski differential interference contrast optics under near-infrared illumination. RGCs were selected for recording by targeting cells with soma >10 μm (Vaney 1980) and lying proximal to the inner limiting membrane.

Electrodes were pulled from borosilicate glass with outer and inner diameters of 1.5 and 0.86 mm, respectively. All electrodes were coated with Sylgard (Dow Corning) and flame polished before use. For whole cell recordings electrodes were filled with an intracellular (pipette) solution containing (in mM): 116 $KMeSO_4$, 10 KCl, 0.5 EGTA, 1 $MgCl_2$, 10 HEPES, 4 ATP-Na_2, 0.5 GTP-Na_3, adjusted to pH 7.2 with KOH. The electrodes had resistance 3–6 MΩ with this solution. To study RGC spikes due to direct activation, in some recordings synaptic transmissions were blocked with 250 μM $CdCl_2$. Tetrodotoxin (TTX) at 1 μM was used to block RGC spikes. In both cases, the pharmacological agents were added directly to Ames' medium and perfused over the retina. All chemicals were acquired from Sigma–Aldrich.

No systematic difference was found for electrical elicitation thresholds between the cell-attached mode and whole cell mode recording techniques. We thus pooled the results from both techniques during analysis.

Data analysis

Spikes were detected using pCLAMP10 (Molecular Devices) with threshold crossing. Data were analyzed with UNIX command line utilities on MacOS X (Apple), MATLAB (The MathsWorks), and Prism (GraphPad Software). The statistical tests used will be stated as they appear. The confidence level has been set at 95% (two-tailed).

Fitting of direct RGC elicitation probability to stimulus strength

Assuming that direct elicitation of RGC spikes was due to activation of independent voltage-gated channels by the stimulus, we used the following Boltzmann equation to describe the probability of eliciting RGC spikes as a function of stimulus current amplitude, in accordance with Hodgkin–Huxley style analysis of neural excitation

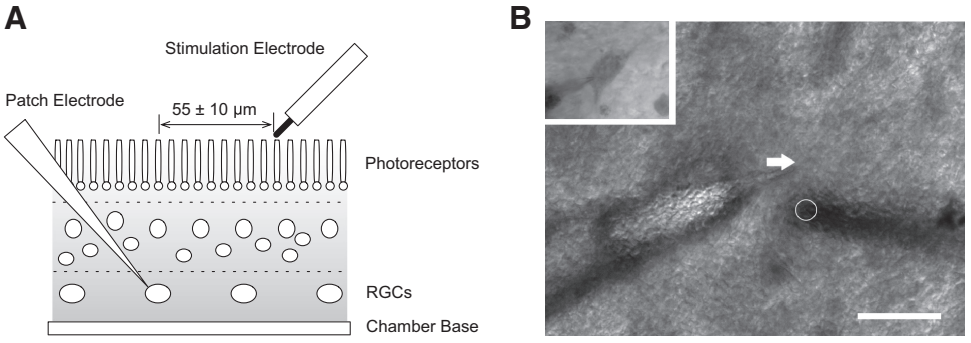

FIG. 1. Typical subretinal stimulation configuration. *A*: a schematic diagram of the stimulation and recording arrangement. The whole-mount retina was placed photoreceptor side up on an inverted microscope. The 25-μm platinum–iridium (Pt-Ir) stimulation electrode was placed at the photoreceptor side under visual guidance to a lateral distance of 55 ± 10 μm from the soma of the targeted retinal ganglion cell (RGC). *B*: a photograph (×100 magnification) of the setup. The arrow marks the location of the cell and the circle denotes the point of contact of the stimulation electrode at the photoreceptor-side. Scale bar = 100 μm. *Inset*: view (×400 magnification) of the targeted RGC.

$$P(I) = \frac{100}{1 + e^{-(I-\alpha)/\beta}}$$

where $P(I)$ is the probability of eliciting a spike and I is the applied current as a percentage of the threshold current. The fitting parameters are α and β.

Creation of temporal activity maps

To quantitatively assess the time series data recorded from RGCs in electrically stimulated retina as a function of stimulus strength, we analyzed the homogeneity of repeated stimulation runs against the corresponding repeated control runs without stimulus presentation. We begin here by formally defining the methodology for the general case.

Assuming weak stationarity, the time series data were first decomposed into orderly stochastic point processes. Let $\mathbf{S}$ and $\mathbf{C}$ be the set of trials with and without stimulus presentation, respectively. The trials were indexed $k = 1, \ldots, K$, so that $k = 1$ for the first trial, and $k = K$ for the last trial. For each trial we had the recording interval $(0, T]$, where T is the recording duration. Recording intervals were divided into small equal segments each with duration Δt and indexed as $n = 1, \ldots, N$, such that $T = N\Delta t$. So we may denote a particular segment for a particular trial in the stimulation set as $\mathbf{S}_{k,n}$ and similarly for the control set as $\mathbf{C}_{k,n}$. We chose Δt to be sufficiently small such that each interval of each trial contained either one spike or no spike. Thus a 2×2 contingency table could be constructed for the following pairs, for each segment n

$$S_n = \bigcup_{k=1}^{K} S_{k,n}$$

$$C_n = \bigcup_{k=1}^{K} C_{k,n}$$

With this formalization we then statistically tested each segment with stimulus presentation $\mathbf{S}_n$ against its corresponding segment without stimulation $\mathbf{C}_n$ (the control) for homogeneity using Fisher's exact test (two-tailed, 95% CI).

In practice, unless stated otherwise, we performed 20 repetitions for both the control trials and the stimulation trials ($K = 20$), with each trial having a duration of 100 ms ($T = 100$). The control trials were always performed before the stimulation trials. Based on previous reports of RGC firing frequency (O'Brien et al. 2002) and our observations, the segments were set to 2 ms ($\Delta t = 2$), such that all segments contained either one spike or none.

The results are presented here as bivariate figures with the horizontal axis being the time and the vertical axis being the stimulation parameter (see Fig. 6 for example). A star symbol (*) marks all segments where the difference from the control is statistically significant at the 95% confidence level. The colors indicate the spiking probability for a given time segment aggregated over 20 repetitions with identical stimulus, expressed as a percentage. Therefore a value of 100 at a particular time segment would indicate that every stimulus presentation successfully elicited a spike within that time interval. In this report we call these figures "temporal activity maps."

RESULTS

Subretinal stimulation could elicit short-latency direct RGC responses

To study the effects of subretinal electrical stimulation on the retina, we placed a stimulation electrode at the photoreceptor side such that its tip visibly contacted the distal boundary of the photoreceptor layer, as depicted schematically in Fig. 1*A*. A photograph of the typical configuration viewed from the RGC side at ×100 magnification is shown in Fig. 1*B*. The cell is marked with an arrow and the circle denotes the position of the stimulation electrode at the photoreceptor side. The *inset* shows the targeted RGC, which has been labeled with Azure B.

Using cell-attached or whole cell current-clamp recordings we found that with sufficient stimulus strength subretinally placed electrodes were able to elicit short-latency stimulus-locked action potential(s) in almost all (97.9%) RGCs tested ($n = 46/47$). Importantly, these responses were easily distinguished from the stimulus artifacts. Figure 2*A* shows ten superimposed cell-attached recordings of an OFF–RGC on stimulation with a 125-μA, 0.1-ms biphasic pulse. Six of the ten trials elicited an action potential. As shown in the *inset* of Fig. 2*A*, these short-latency spikes were blocked by TTX (1 μM, $n = 3/3$ cells). Spike responses were equally clear with long-duration stimuli. In Fig. 2*B* an OFF–RGC was successfully activated in seven of the ten trials using a 7-μA, 5.0-ms biphasic pulse. The spike latency and temporal jitter were larger than those for 0.1-ms pulses in Fig. 2*A*. Also apparent in both figures are spontaneous spikes not correlated to the electrical stimuli. As demonstrated in Fig. 2*C*, these stimulus-locked short-latency responses remained in the presence of bath-applied $CdCl_2$ (250 μM, $n = 7/7$ cells). This suggests that they were not of presynaptic origin.

Taken together, these results indicated that subretinal stimulation could reliably activate RGCs directly, evoking short-

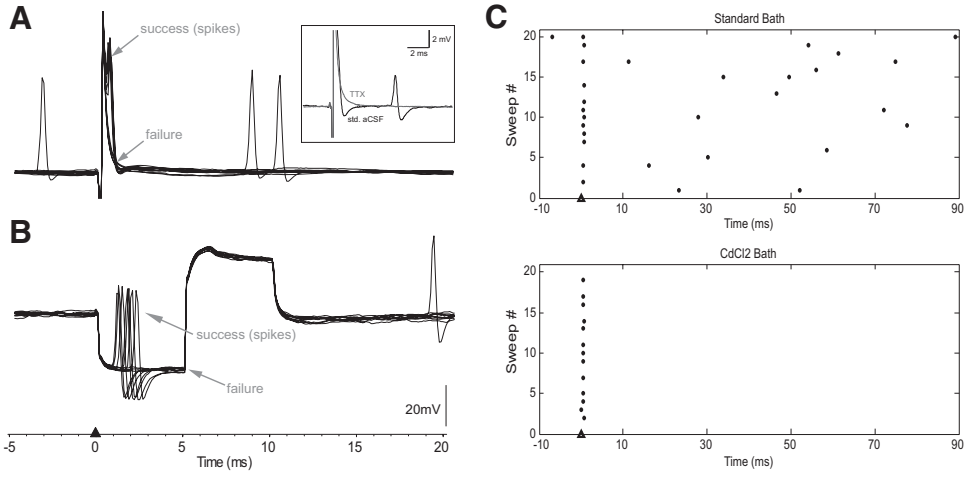

FIG. 2. Elicitation of short-latency stimulus-locked RGC responses with subretinal stimulation. *A*: 10 superimposed traces of an OFF–RGC stimulated with a single 125-μA, 0.1-ms biphasic pulse delivered at the 0-ms time point. Six of the trials successfully elicited a short-latency spike, which was clearly distinguished from the biphasic stimulus artifact. *Inset*: short-latency responses were blocked by tetrodotoxin (TTX, 1 μM, $n = 3/3$). *B*: 10 superimposed traces of an OFF–RGC stimulated with a 7-μA, 5.0-ms biphasic pulse. A short-latency response was elicited in 7 trials. These spikes were also easily seen within the artifacts. *C*: raster plots of a cell stimulated 20 times with a 105-μA, 0.1-ms pulse. The short-latency responses remained in the presence of $CdCl_2$ (250 μM, $n = 7/7$), suggesting that they were not of presynaptic origin.

latency stimulus-locked responses that were visible with cell-attached and whole cell current-clamp recordings.

Thresholds of short-latency direct RGC responses

To determine the threshold of these short-latency spikes we recorded from ON ($n = 14$), OFF ($n = 23$), and ON–OFF ($n = 5$) cells over pulse durations 0.1–5.0 ms. Figure 3 summarizes the results for these cells. For all cell types the threshold decreased with increasing pulse width. However, there was no statistically significant difference in thresholds between the cell types for eliciting short-latency direct activation responses with subretinal stimulation (two-way ANOVA, $P = 0.6561$).

Figure 4 shows the charge densities on the 25-μm Pt-Ir electrode at the median threshold for eliciting short-latency stimulus-locked spikes over pulse widths 0.1–5.0 ms. The data from all cell types (ON, OFF, ON–OFF; $n = 42$) have been pooled for the calculation. The median charge density was lowest with 0.2-ms pulses, at 1.43 mC/cm^2, and increased with pulse width $\geq$0.2 ms.

RGC activation probability increased nonlinearly with stimulus strength

We examined the probability of eliciting direct RGC responses with respect to the variation in stimulation strength. Using 20 consecutive trials of 0.1-ms biphasic pulses on 12 cells ($n = 4$ for each of ON, OFF, ON–OFF) we determined the percentage of trials with successful activation against the stimulus strength, expressed as a percentage of the cells' threshold current (Fig. 5).

The fitting parameters in the Boltzmann equation, their corresponding confidence intervals, and the goodness-of-fit measures are listed in Table 1. For all three RGC types investigated the probability of activation increased nonlinearly with stimulus current. In all cases there was a critical current range in which the chance of directly evoking RGC spikes rose dramatically with increasing stimulus amplitude. Below or above this region the rate of increase was markedly reduced.

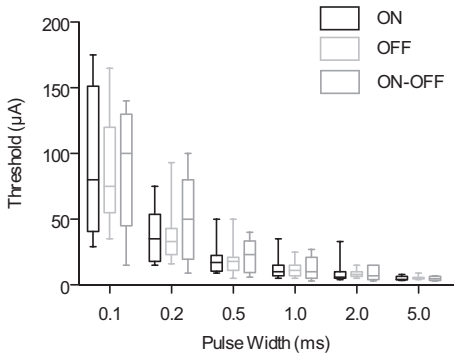

FIG. 3. Strength–duration plot for short-latency direct RGC activation. The thresholds for ON ($n = 14$), OFF ($n = 23$), and ON–OFF ($n = 5$) cells were determined for pulse widths 0.1–5.0 ms. The median current amplitude reduced for all cells with increasing pulse width. No significant difference was found for the thresholds between the 3 cell types over the pulse widths tested (2-way ANOVA, $P = 0.6561$). The box-and-whisker plot shows (from *top* to *bottom*) the maximum, third quartile, median, first quartile, and minimum.

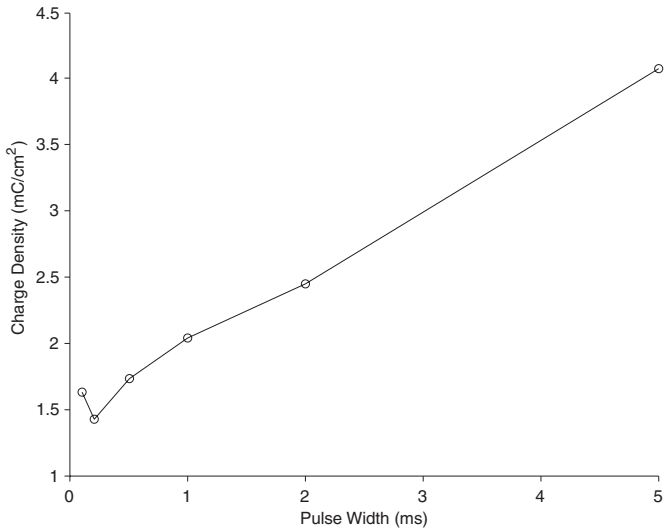

FIG. 4. Charge density for direct activation of RGCs. The median charge density was lowest with 0.2-ms pulses and increased with pulse width thereafter. The data from all cell types (ON, OFF, and ON-OFF; $n = 42$) have been combined in this graph.

Temporal response properties of RGCs were cell and stimulus strength dependent

In addition to the short-latency stimulus-locked spikes detailed thus far, subretinal stimulations generally also evoked responses with longer latencies, some in the order of tens of milliseconds or more. We attempted to gain a quantitative understanding of how the stimulus strength modulated both of these response types. Temporal activity maps were created from the 0.1-ms biphasic stimulation data sets for all RGCs. The electrical stimuli were always delivered at the 0-ms time point. In all maps stimulus strength is shown on the vertical axis and time progresses from left to right. We found the temporal response profiles of RGCs following subretinal stimulation to be highly heterogeneous. The responses varied between cells and for a given cell generally also varied with stimulus strength. This is demonstrated with the temporal

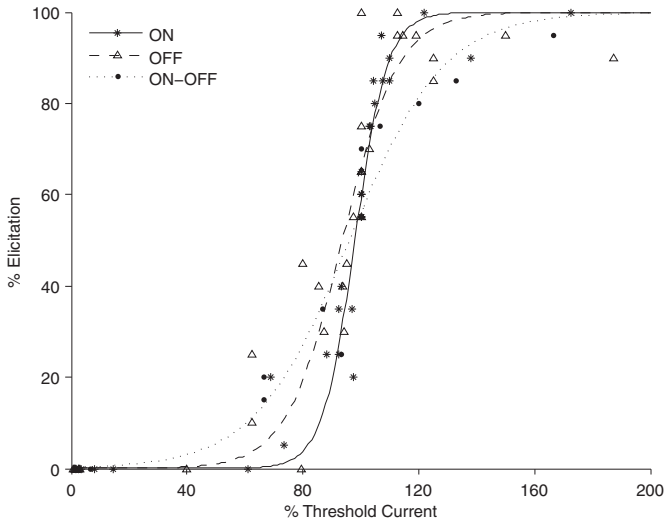

FIG. 5. Modulation of elicitation probability with current amplitude. The probability of eliciting short-latency RGC responses increased nonlinearly with stimulus strength. Boltzmann curves were fitted to the data points for each cell types ($n = 12$).

TABLE 1. *Relationship between spiking probability and stimulus amplitude*

Cell Type	α (95% CI)	β (95% CI)	R^2	RMSE
ON	98.0 (96.8, 99.2)	5.6 (4.2, 6.9)	94.5%	8.6
OFF	93.7 (90.7, 96.6)	9.6 (6.1, 13.0)	98.5%	12.2
ON–OFF	96.1 (90.6, 101.6)	16.2 (9.5, 22.9)	93.9%	8.9

The relationship between spiking probability and stimulus current, expressed as a percentage of threshold, can be described by a Boltzmann curve. The fitting parameters and 95% confidence intervals are shown here. Also listed are the goodness-of-fit measures.

activity map of four cells in Fig. 6. It should be emphasized that the temporal activity patterns presented here are not exhaustive.

In some cells electrical stimulation elicited only a single short-latency spike. Besides enhancing the presence of these responses, further increase of the stimulation current had no other statistically significant effect on spiking activities. Figure 6*A* shows an example of such cells. The probability of eliciting short-latency spikes increased with the current amplitude. Of all 2-ms time segments immediately after stimulus presentation, only the 70- and 75-μA cases were statistically different from the control without stimulus delivery.

Electrical stimulation had a suppressive effect on the spontaneous activities of some cells. As demonstrated in Fig. 6*B*, by using current $\geq$70 μA, the spiking activities of this cell were sufficiently reduced around the 36-ms time point such that the differences compared with the control were statistically significant. The threshold for initiating this suppressive effect (70 μA) was higher than the threshold for eliciting short-latency spikes (65 μA). Both the short-latency responses and the spike suppression persisted for current $>$75 μA (data not shown).

The cell in Fig. 6*C* exhibited spikes with three categories of latency: $<$2 ms, 4–6 ms, and $>$35 ms. Their occurrences were stimulus strength dependent. Although activities of all categories were apparent at 80 μA, only the segments belonging to the second category were statistically different from the control. Increasing the current further made the second category spikes more robust. The presence of the third category became significant at 90 μA. The first category, with latency $<$2 ms, had the highest threshold at 95 μA.

Somewhat similar is the cell in Fig. 6*D*, which exhibited two categories of response latency, one of $<$2 ms and another with $>$33 ms. Stimulating at 100 μA elicited a cluster of long-latency spikes at the 50- to 60-ms time points. The presence of short-latency responses became statistically significant at 125 μA. Thus this is the opposite of Fig. 6*C*, where short-latency responses had a lower threshold than that of the long-latency responses. Further increase of stimulus strength raised the probability of eliciting both the short-latency responses and the long-latency spike cluster.

We did not observe any correlation between the RGC types (ON, OFF, ON–OFF) and the temporal response patterns elicited by electrical stimulation. In summary, the temporal activity profiles of RGCs following subretinal stimulation varied from cell to cell. Furthermore, for a given cell the responses were dependent on stimulus strength.

Classification of RGC temporal response profiles

Although the temporal responses of RGCs following subretinal stimulation were heterogeneous, we found that the responses could be generalized into four classes: primary

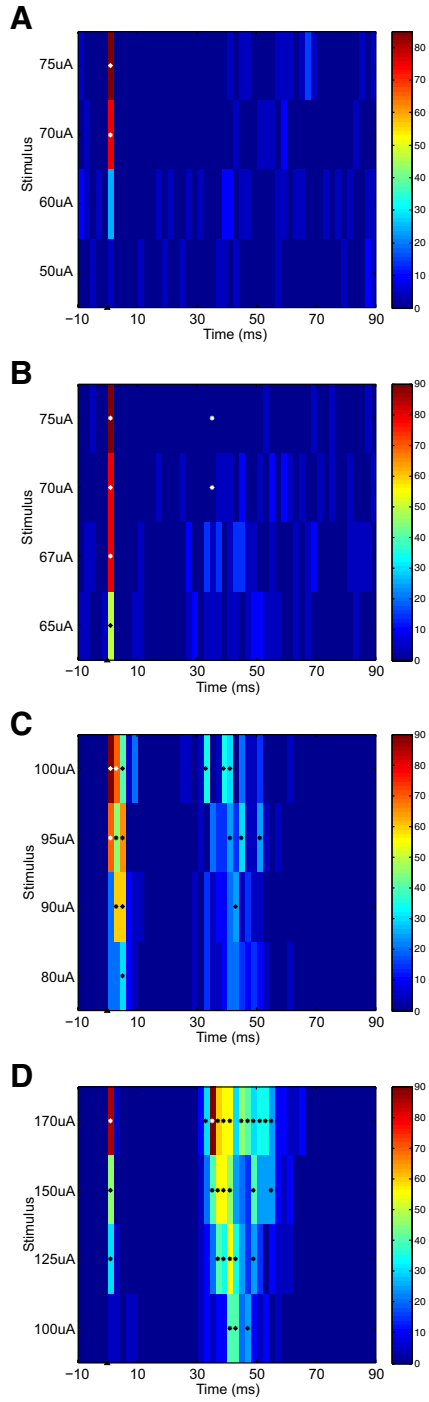

FIG. 6. Temporal activity map of 4 RGCs stimulated with 0.1-ms biphasic pulses. The color in each time segment indicates the response rate (%), over 20 consecutive trials. Stars mark all segments statistically different from the control (without stimulus). *A*: a cell that exhibited only short-latency responses. *B*: an example of a cell that had a period of reduced activity in addition to the short-latency responses. *C*: a cell that exhibited 3 classes of responses with different latencies (in order of increasing threshold): 4–6, $>$40, and $<$2 ms. *D*: similar to the previous cell, but with only 2 classes of response, one with latency $>$40 ms and another with latency $<$2 ms.

TABLE 2. *Properties of the four RGC temporal response classes following subretinal stimulation*

Response Class	Latency, ms	Duration, ms	Frequency
Primary spike	≤2	1 spike	98%
Secondary spike(s)	4–20	1–2 spikes	36%
Latent period	2–45	2–30 ms	11%†
Late onset cluster	25–50	10–40 ms	15%

The values here are based on data from stimulation of RGCs with 0.1-ms pulses.† See text for details.

spike, secondary spike(s), latent period, and late onset cluster. Together these classes completely described the responses of every RGC studied. The temporal activity maps of RGCs following 0.1-ms biphasic pulse stimulation were used to quantitatively identify and categorize the response patterns. Table 2 summarizes the pertinent features of the four response classes when RGCs were stimulated with 0.1-ms pulses. Also listed is the prevalence of each class in our sample of RGCs.

Primary spikes had response latency of ≤2 ms and showed little temporal jitter (Fig. 7). These were the short-latency, stimulus-locked action potentials described earlier. Almost all RGCs studied exhibited this class of response (n = 46/47). Pharmacological blocking of synaptic inputs with $CdCl_2$ suggested that these spikes were not of presynaptic origin (Fig. 2*C*). Increasing the stimulus amplitude increased the probability of eliciting this response.

The secondary spike(s) class consisted of either one or two action potentials. The onset latencies were 4–20 ms and had more temporal jitter than that of the primary spikes. This is demonstrated by the raster plot of a cell with both classes of response (Fig. 7*A*). The latency range (Fig. 7*B*) of the secondary spikes was longer than that of the primary spikes. Furthermore for cells exhibiting secondary spikes, the threshold for these responses could be lower than, higher than, or equal to the threshold of the primary spikes. The secondary spikes of the cell in Fig. 6*C* provide an example of the first case. Secondary spikes were observed in 17 of 47 cells. Applications of $CdCl_2$ (250 μM) abolished spikes of this response class in all cells examined (n = 3/3), indicating that these were likely to be of presynaptic origin. This class of response became more robust with increasing stimulus amplitude.

The latent period was characterized by a time interval within which the RGC spiking activity was significantly lower than that of the control. The onset latencies were variable (4–20 ms). The observed durations ranged from 2 to 30 ms for the stimulus current levels tested. Only five RGCs (n = 5/47) displayed this class of response. However, the present statistical comparison technique may have underestimated the actual prevalence of this response class (see DISCUSSION).

The late onset cluster class encompassed the spike cluster with latencies of 25–50 ms (calculated to the first spike of the cluster). The durations were variable, ranging from 10 to 40 ms. In some cases (n = 3) the durations were stimulus strength dependent, increasing with pulse duration. The threshold for eliciting this response could be higher (Fig. 6*C*) or lower (Fig. 6*D*) than the primary and secondary spike classes. Of the cells examined, seven (n = 7/47) had this class of response.

Using data from all three cell types (ON, OFF, and ON–OFF; n = 42 cells), we compared the thresholds for eliciting primary spikes, secondary spikes, and late onset clusters (Fig. 8). There was no systematic difference in thresholds of these response classes over the pulse width tested (two-way ANOVA, P = 0.071).

Long stimulus pulses increased latency and onset jitter of primary and secondary spikes

Using temporal activity maps of RGCs stimulated with 0.1-ms pulses, we have shown that the temporal response profiles could be generalized into four classes despite the observed diversity both within and between cells. However, the question arises whether RGC responses were also pulse width dependent (in addition to being pulse amplitude dependent, as demonstrated earlier) and, more generally, whether the proposed response classification scheme is valid for long-duration electrical stimuli.

We began by comparing the temporal activity maps of stimulation trials over pulse widths 0.1, 1.0, and 2.0 ms for each RGC. In general, the temporal response characteristics for each cell were preserved across pulse widths. Thus if a cell demonstrated (or lacked) particular temporal response classes when stimulated with 0.1-ms pulses, then the same response classes would also be present (or absent) at longer stimulus pulses. Figure 9 shows the temporal activity maps of three cells (Fig. 9, *A* and *B*; *C* and *D*; and *E* and *F*) stimulated with 0.1- and 2.0-ms pulses. The primary spikes remained as the pulse width was increased. Furthermore, consistent with the observations of Fig. 6, the probability of eliciting primary spikes increased with stimulus strength for all three cells at both pulse widths. Nevertheless, even with 2-ms time segments the increase in temporal jitter due to longer pulses was readily

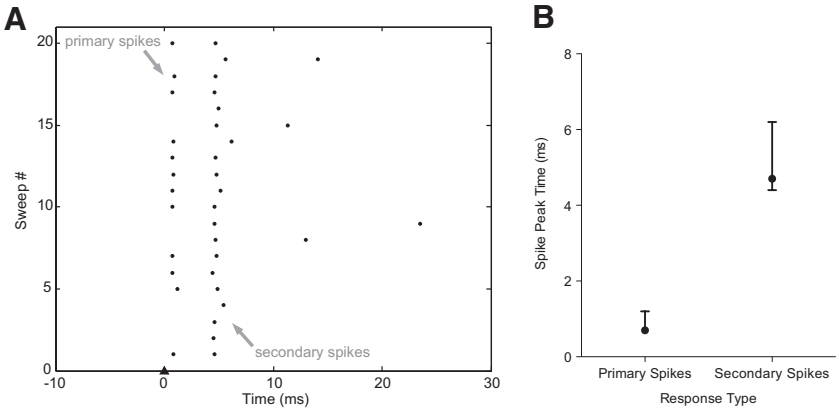

FIG. 7. Jitter comparison of the primary and secondary spikes. *A*: raster plot of a cell stimulated with 150-μA, 0.1-ms biphasic pulses. The primary spikes had latency ≤2 ms after stimulus onset, whereas the secondary spikes had latency of 4.4–6.2 ms. *B*: the median latency and range of the 2 response classes in the raster plot. The secondary spikes exhibited larger temporal jitter than the primary spikes.

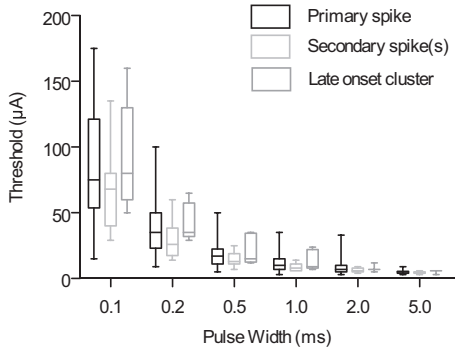

FIG. 8. Thresholds of RGC response classes: primary spike, secondary spike(s), and late onset cluster. For all response classes the threshold decreased with pulse width. However, there was no systematic difference in threshold between the classes over the pulse widths tested ($n = 42$; 2-way ANOVA, $P = 0.071$).

apparent in two of the three cells. In the first (Fig. 9, *A* and *B*) and second (Fig. 9, *C* and *D*) cells, onset of the primary spikes was delayed by one time segment (2 ms) when the stimulus pulse width was increased from 0.1 to 2.0 ms.

To further investigate the effect of pulse width on RGC spiking responses, we compared the latencies of the primary and secondary response classes as a function of pulse widths. Plotted in Fig. 10*A* are the median and range of RGC primary spike latencies for pulse widths (ms): 0.1, 1.0, and 2.0, when the cells ($n = 12$) were stimulated at the threshold for primary spikes. The differences in median latencies were highly significant (Kruskal–Wallis, $P < 0.0001$). The median latency of 0.1-ms pulses was significantly different from the median latency of 1.0- and 2.0-ms pulses (Dunn's posttest, $P < 0.05$). Also apparent in the figure is the increase in temporal jitter of the response spikes, as indicated by the increased interquartile ranges, when longer stimuli (1.0 and 2.0 ms) were used. The differences in latency variance between those elicited by 0.1-ms stimuli and the longer stimuli were highly significant (Levene's test; 0.1 vs. 1.0 ms, $P < 0.001$; 0.1 vs. 2.0 ms, $P < 0.001$).

Figure 10*B* shows the median and range of RGC ($n = 9$) secondary spike latencies for pulse widths (ms): 0.1, 1.0, and 2.0. For cells that responded with more than one secondary spike, we used the time-of-peak of the first spike to calculate the latency. The median latency increased significantly with pulse width (Kruskal–Wallis, $P < 0.0001$, Dunn's posttest, $P < 0.05$). By comparing Fig. 10*A* with 10*B* it is also apparent that the temporal jitter of primary spikes was smaller than that of the secondary spikes at all pulse widths tested.

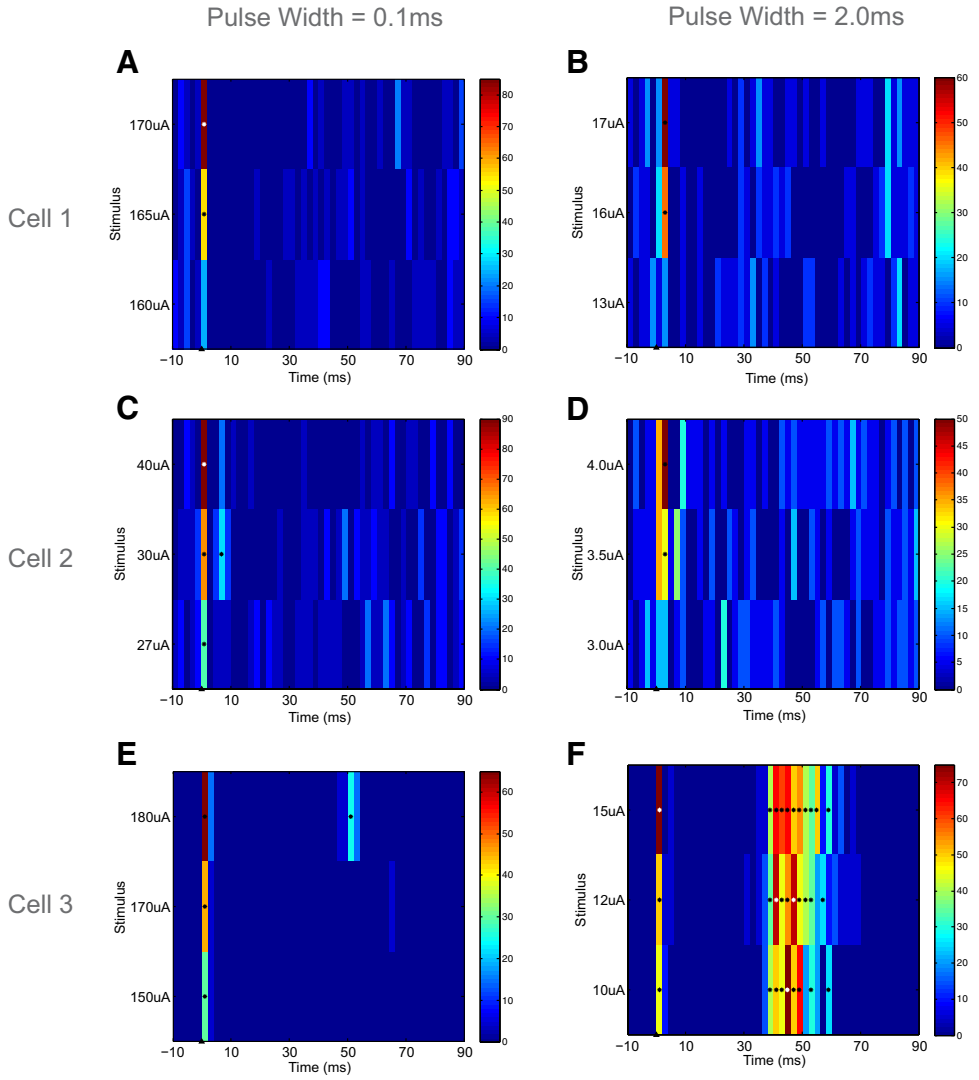

FIG. 9. Comparison of temporal activity maps of RGCs stimulated with 0.1- and 2.0-ms pulses. Shown here are the temporal activity maps of 3 RGCs stimulated with 0.1-ms (*left column*) and 2.0-ms (*right column*) biphasic pulses. The temporal response characteristics were preserved across different pulse widths. However, long-duration pulses generally increased the response latencies, as apparent from the temporal activity maps of the first (*A* and *B*) and second (*C* and *D*) cell.

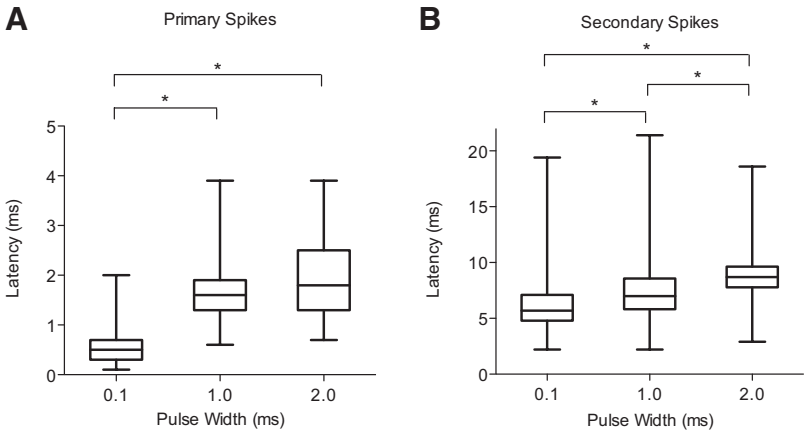

FIG. 10. The effect of pulse width on the latency of primary and secondary spikes. *A*: the median latency of primary spikes elicited by 0.1-ms stimulus pulses was significantly shorter than that by 1.0- and 2.0-ms pulses ($n = 11$; Kruskal–Wallis, $P < 0.0001$, Dunn's posttest, $P < 0.05$). The jitter of spike onset also increased with pulse width. The latency variances of responses elicited by the 0.1-ms pulses were significantly different from those elicited by longer pulses (Levene's test; 0.1 vs. 1.0 ms, $P < 0.001$; 0.1 vs. 2.0 ms, $P < 0.001$). *B*: the increase in median latency of secondary spikes due to increasing pulse width was significant ($n = 9$; Kruskal–Wallis, $P < 0.0001$, Dunn's posttest, $P < 0.05$).

In summary, the four temporal response classes remained valid for long-stimulus pulses. However, some characteristics of the response classes varied with stimulus pulse width. In the case of the primary spikes, increasing the pulse width increased the median latency and temporal jitter. For the secondary spikes, we observed an increase in median latency with increasing pulse width.

Depression of RGC primary spikes by repetitive stimulation

Given the prolonged activities of many RGCs subsequent to a single subretinally applied electrical stimulus, as apparent from the temporal activity maps, and the presence of primary spikes in almost every cell investigated, we asked whether this class of response could be reliably elicited during repetitive stimulations using the subretinal paradigm. We performed repetitive stimulations on RGCs ($n = 11$) with a pulse train consisting of four identical biphasic stimuli. For each cell, four pulse train frequencies were tested (50, 66.7, 100, and 200 Hz) and, at each frequency, three different stimulus pulse widths were tested (0.1, 0.2, and 0.5 ms).

Figure 11*A* shows the mean primary spike response rate (%) of the cells to each of the four 0.1-ms pulses over 20 repetitions. The results for all four stimulation frequencies are presented together. Figure 11, *B* and *C* illustrates the results for pulse width of 0.2 and 0.5 ms, respectively. For all stimulus frequencies and every pulse width tested there was a trend for decreasing response rate with repetitive stimulation. The differences in response rate to the pulses in the stimulus train were significant (repeated-measures two-way ANOVA) for all pulse widths tested (0.1 ms, $P < 0.0001$; 0.2 ms, $P = 0.0059$; 0.5 ms, $P = 0.0005$). However, for a given pulse width, there was no significant difference in response rate among the four stimula-

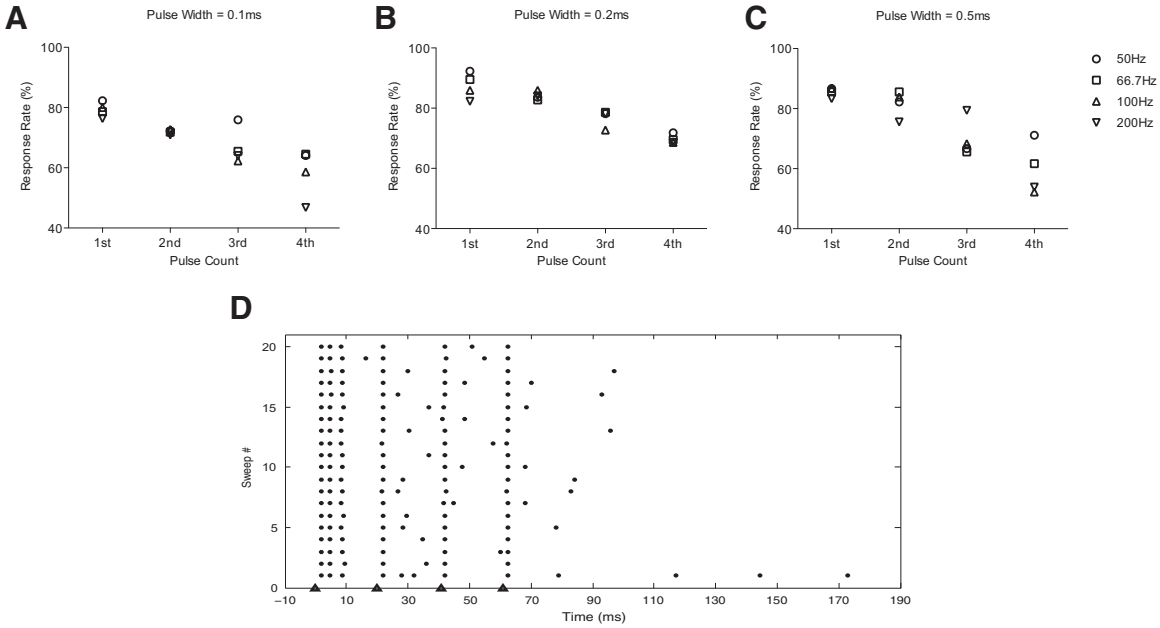

FIG. 11. The response rate of RGC spikes reduced with repetitive subretinal stimulation. There was a trend for decreasing response rate with each subsequent stimulus pulse. For all pulse widths and all repetition frequencies, the differences in primary spike response rate between each successive pulse in the train were statistically significant ($n = 11$; repeated-measures 2-way ANOVA). However, given a pulse width, there was no significant difference between the stimulation frequencies tested. *A*: four 0.1-ms pulses, between pulses: $P < 0.0001$; between frequencies: $P = 0.4200$. *B*: four 0.2-ms pulses, between pulses: $P = 0.0059$; between frequencies: $P = 0.7429$. *C*: four 0.5-ms pulses, between pulses: $P = 0.0005$; between frequencies: $P = 0.8154$. *D*: raster plot of a cell exhibiting both primary and secondary spikes when the cell was stimulated at 50 Hz with 4 identical 0.1-ms biphasic pulses. The secondary spikes were less robust than the primary spikes.

tion frequencies (0.1 ms, $P = 0.4200$; 0.2 ms, $P = 0.7429$; 0.5 ms, $P = 0.8154$).

These results suggested that repetitive subretinal stimulation increased the failure rate of eliciting RGC primary spikes. This was true for all pulse widths tested. Furthermore, the response rates were not significantly different between the slowest repetition frequency (50 Hz) and fastest repetition frequency (200 Hz) attempted.

Four of the cells ($n = 4/11$) also exhibited secondary spikes when stimulated with a single biphasic stimulus. Shown in Fig. 11*D* is one of the cells stimulated at 50 Hz with four 78-μA, 0.1-ms biphasic pulses. Primary spikes were successfully elicited (100%) for all four stimuli during the trial. The first stimulus also elicited secondary spikes in all 20 trials. However, the response rate of secondary spikes diminished faster than those of the primary spikes with each subsequent stimulus. This was observed in all four cells for all pulse widths at all repetition rates. This suggests that, in our sample of RGCs, secondary spikes were less robust during repetitive stimulation than the primary spikes.

DISCUSSION

Using cell-attached and whole cell current-clamp recordings this report investigated the responses of rabbit RGCs to subretinal stimulation with small-diameter electrodes.

Activation of RGCs with subretinal stimulation

Subretinal stimulation could elicit RGC responses directly. The effects of subretinal stimulation on RGCs have been studied by several investigators using a variety of species, including: frogs (Li et al. 2005), chickens (Stett et al. 2000), rabbits (Jensen and Rizzo 3rd 2006, 2007; Shyu et al. 2006), and mice (Jensen and Rizzo 3rd 2008; O'Hearn et al. 2006). However, previous reports have not provided conclusive evidence for the existence of short-latency responses (primary spikes) with subretinal stimulation. The reason for this may be due to the recording techniques used. In all previous studies RGC responses were recorded extracellularly with metal or carbon-fiber electrodes. Large stimulus artifacts, lasting several milliseconds or more, have been observed in these studies.

Shyu et al. (2006) were unable to elicit RGC responses consistently with 25-μm-diameter electrodes for pulse widths $<$1.0 ms, when the electrodes were placed either subretinally or epiretinally. We were able to evoke short-latency direct responses in all but one of the RGCs. For this cell the highest current amplitude tested at 0.1 ms was 200 μA, the maximum output of our stimulator. At this level the cell clearly exhibited responses belonging to the secondary spike(s) class. This cell may have had an unusually high threshold for primary spikes. It is possible that we would have evoked short-latency responses had we been able to deliver higher currents with the stimulator.

Threshold of direct RGC activation. Attempts to compare the present thresholds to previous reports are confounded by several factors. First, in a number of previous subretinal stimulation studies the activation thresholds were not systematically investigated or reported, whereas others have used voltage stimuli or monophasic current pulses. Second, we have noted that subretinal stimulation gives rise to four classes of RGC responses. Earlier reports have not distinguished between these different classes and reported thresholds as the current levels that evoked the first instance of any one or more of the RGC response classes. Due to their prevalence and for consistency we have reported the threshold for eliciting primary RGC spikes. As noted previously, the threshold for these responses for a given cell could be higher than, lower than, or equal to the threshold of any of the other response classes. Third, existing subretinal reports have not been able to unambiguously resolve the short-latency stimulus-locked responses, potentially biasing the reported thresholds. Last, thresholds have not been defined consistently in the literature. Some investigators have used the definition as the current required for evoking RGC responses in 50% of the trials, whereas others used the definition as the current needed for successfully eliciting spikes in 90% of the trials. However, in practice this may not be a significant issue. Figure 5 shows that, at least for ON and OFF type RGCs, within the current range required for eliciting direct RGC responses in 20–80% of the trials, a small increase in stimulus amplitude resulted in a disproportionally large increase in probability of evoking responses.

Quantitative assessment of RGC temporal response profiles

The primary spikes were characteristically conspicuous and thus easily correlated with the stimuli. The other response classes were more difficult to assess in relation to the stimulus parameters. We statistically analyzed the time series data to ensure that the presence of these responses was above chance and stimulus driven. We found assessment on the basis of raster plots and peristimulus time histograms, as has been done previously, to be subjective and thus unreliable. This is especially true when evaluating the latent periods and late onset clusters, resulting from their large temporal jitter of onset and variability in duration.

It should be noted that the temporal activity maps used spikes to analyze differences between two time series data sets. Therefore the accuracy of this technique in measuring spike inhibition due to electrical stimulation relied on the cell having some level of sustained spontaneous activities. The median spontaneous firing rate of the RGCs in our study was 4.5 Hz (approximately Poisson distribution; with 52% of cells $\leq$4 Hz), which is equivalent to 0.45 spike per 100 ms. The temporal activity maps were divided into 2-ms time segments. Thus in general the segments would be very sparse under the control condition. For this reason, the true prevalence of the latent period could have been underestimated.

Efficacy and safety of subretinal stimulation

Temporal accuracy of RGC spikes. To simulate natural-light responses, vision prostheses should be capable of eliciting spikes over a wide range of frequencies. Jensen and Rizzo 3rd (2008) previously reported that RGC response rate declined with each successive pulse when stimulating subretinally at frequencies $\geq$4 Hz and that most RGCs did not respond to frequencies $\geq$60 Hz. Their response latencies were of the order of 5–32 ms and thus most likely the equivalent of our secondary spikes and possibly also the late onset clusters. Our results indicated that, in addition to a reduction of secondary spike response rate (Fig. 11*D*), there was also a decreasing trend in

response rate of the primary spikes during repetitive subretinal stimulation at all frequencies tested (Fig. 11, *A–C*). However, with the exception of the 0.1-ms, 200-Hz case, the response rates of all other configurations were still >50% (above threshold) by the fourth pulse. The stimulation frequencies used in the present study were also much higher (50–200 Hz). These results suggest that the primary spikes were less susceptible to repetitive stimulation failure than the other response classes. Margalit and Thoreson (2006) and Fried et al. (2006) previously found that activation of the amacrine cells resulted in a large sustained inhibitory postsynaptic current (IPSC) lasting ≥500 ms, which suppressed RGC excitability. Compared with the IPSC, bipolar cell excitatory postsynaptic currents (EPSCs) were of smaller amplitude and duration. Presumably then, when RGC spikes were repetitively evoked via stimulation of the presynaptic pathway during subretinal stimulation, the inhibition by amacrine cells onto the bipolar cells and the RGCs far outweighed the excitatory inputs from the bipolar cells. Thus the RGCs were unable to follow high-frequency stimulation. However, when the RGCs were recruited directly (Ahuja et al. 2008; Fried et al. 2006; Sekirnjak et al. 2006), spiking responses of the RGCs no longer depended critically on the bipolar cell inputs, thus making repetitive stimulation more robust than the scenario involving elicitation via the network. Taken together, the results suggest that to achieve reliable activation during repetitive stimulation >4 Hz, subretinal vision prostheses may need to activate RGCs directly, rather than through activation of the retinal network.

Electrical stimulation of the retina should ideally elicit responses with high temporal precision. This will be particularly important during high-frequency stimulation. It is apparent in Fig. 10 that short pulses resulted in shorter response latencies and for the primary spikes also smaller temporal jitter of onset. Therefore short pulses would be preferred in this context.

Selective excitation of RGCs. To imitate natural-light responses, retinal stimulation should ideally excite the RGCs selectively. We did not observe any significant difference in threshold when classifying RGCs on the basis of ON, OFF, and ON–OFF types. This is consistent with previous findings using biphasic stimuli (Sekirnjak et al. 2008). We also did not find any correlation between the light response properties (ON, OFF, ON–OFF, transient/sustained and peak firing rate) and the resulting electrical response classes evoked on the RGCs (data not shown). Fried et al. (2009) found the difference in threshold between brisk transient cells, direction selective cells, and local edge detectors to be significantly different when stimulating epiretinally. However, the light stimulus used here did not allow us to functionally distinguish between RGCs to the same extent as in their study.

Safety. Although small electrodes in theory provide more focused stimuli, the charge density has to remain within the safety limit of the electrodes for chronic applications. It can be seen in Fig. 4 that, except for the slight increase with 0.1-ms pulses, short pulses had lower charge density than that of the long pulses. Since no significant difference in thresholds was observed between the RGC response classes (Fig. 8), this finding also applies for the other spiking response classes. Given the reduced charge density and the higher temporal accuracy mentioned earlier, short pulses are therefore the configuration of choice for subretinal applications.

When stimulating with cathodic first biphasic pulses, the charge injection limits of Pt and Pt-Ir were reported to be 0.7–3.3 mC/cm^2 (Robblee et al. 1983) and, more recently, as low as 0.1–0.15 mC/cm^2 (Brummer and Robblee 1983; Rose and Robblee 1990). Therefore the Pt-Ir electrodes used here would be close to, or even over, the reported limits. To overcome this, one could use electrode materials with higher charge injection limits, such as activated iridium (Brummer and Robblee 1983). Alternatively, larger electrodes may be used. Previous subretinal studies using 125-μm electrodes have found the charge densities to be below the safety limits (O'Hearn et al. 2006; Shyu et al. 2006).

Implications for vision prosthesis design

Comparison of subretinal and epiretinal stimulation. In most aspects the present subretinal findings are similar to those reported for the epiretinal approach using cathodic-first charge-balanced biphasic stimuli. The strength–duration curves (Fig. 3) were comparable; thresholds fell with increasing pulse width (Ahuja et al. 2008; Sekirnjak et al. 2006). The relationship between probability of direct elicitation of RGC responses and stimulus amplitude (Fig. 5) were both sigmoidal (Fried et al. 2009; Sekirnjak et al. 2008). Short-latency responses by direct RGC activation and long-latency responses by stimulation of the retinal network (Table 2) could be elicited in both paradigms (Fried et al. 2006; Sekirnjak et al. 2006). In the epiretinal case, the latency of short-latency responses appeared to be slightly lower on average (approximately ≤0.7 ms). Finally, the responses elicited by direct stimulation of the RGCs were also found to be more robust during high-frequency stimulation than those arising from activation of the retinal network for both subretinal (Fig. 11) and epiretinal (Ahuja et al. 2008; Fried et al. 2006; Sekirnjak et al. 2006) stimulation. In the epiretinal case RGC responses were reliably up to 50 Hz, whereas a moderate decline was noted with subretinal stimulation at the same frequency.

The greatest difference between subretinal and epiretinal stimulation is the minimum electrode size for safe stimulation. It has been demonstrated that epiretinal stimulation using Pt electrodes of 10–15 μm diameter could effectively evoke RGC responses at charge injection densities that were well within the safety limit (0.03 mC/cm^2; Sekirnjak et al. 2006). In contrast, the present subretinally placed 25-μm-diameter electrodes were close to, or over, the safety limit. This implies that, when fabricated from materials such as Pt or Pt-Ir, electrodes placed subretinally are fundamentally more constrained in their minimum size than those placed epiretinally. This may potentially have an impact on the visual resolution achievable on subretinal implants. Furthermore, the lowest charge density required to elicit RGC responses with the present subretinal electrode was about 70-fold higher than the values reported for epiretinal electrodes of comparable dimensions (Sekirnjak et al. 2006). The higher charge density may lead to further loss of focal stimulation.

Further considerations for subretinal implants. There are two methods of eliciting RGC responses with subretinal implants, either through indirect activation by stimulating the retinal network, which has been the primary focus of previous subretinal studies, or through direct stimulation of the RGCs as demonstrated here. Direct activation has a number of advantages over

network stimulation. The response latencies were shorter and had less temporal jitter and, importantly, these responses were more robust during repetitive stimulation. However, spikes evoked via direct activation of RGCs (with high temporal precision) were generally also accompanied by long-latency activity arising from activation of the network (with comparatively poor temporal accuracy). Furthermore, selective excitation of either the RGCs only or the network does not appear to be possible using the present stimulation technique (Fig. 8), due to similarity in thresholds. It is not clear how these long-latency activities will influence the percepts generated initially by direct activation. In contrast, with short-duration pulses and carefully controlled stimulus strength, epiretinal stimulation can be reliably confined to activate only the RGCs (Fried et al. 2006; Sekirnjak et al. 2006).

Experimental considerations

This study investigated the neurophysiological responses of RGCs following electrical stimulation. The complexities of the electrical field associated with the placement of both the working and return electrodes and thus the effect of this field on the retina and the subsequent interpretation of the results were simplified by the use of a monopolar stimulation configuration. Similar to previous in vitro studies, the retinas were isolated and placed in an imaging chamber. The lack of vitreous space and the nonconductive chamber glass base would have influenced the current field arising from the electrical stimuli. This most likely had some impact on the evoked responses.

This study used healthy rabbit retina. The loss of outer neural layers in the diseased retina would bring subretinally placed electrodes closer to the RGCs, thus potentially reducing the activation threshold. However, a high-resistance fibrotic seal forms between the remnant neural retina and the pigment epithelium during disease progression (Marc et al. 2003). This may reverse the benefit of reduced electrode–cell distance. Studies have begun to investigate the activation thresholds of the degenerative retina (Jensen and Rizzo 3rd 2008; O'Hearn et al. 2006), although little is known about the underlying neural mechanisms involved and how these compare with healthy retinas. Future investigations will need to address these issues.

ACKNOWLEDGMENTS

We thank P. Byrnes-Preston for designing and assistance in implementing the neural stimulator.

GRANTS

This work was supported by National Health and Medical Research Council of Australia.

REFERENCES

Ahuja AK, Behrend MR, Kuroda M, Humayun MS, Weiland JD. An in vitro model of a retinal prosthesis. *IEEE Trans Biomed Eng* 55: 1744–1753, 2008.

Amthor FR, Keyser KT, Dmitrieva NA. Effects of the destruction of starburst-cholinergic amacrine cells by the toxin AF64A on rabbit retinal directional selectivity. *Vis Neurosci* 19: 495–509, 2002.

Brummer SB, Robblee LS. Criteria for selecting electrodes for electrical stimulation: theoretical and practical considerations. *Ann NY Acad Sci* 405: 159–171, 1983.

Fried SI, Hsueh HA, Werblin FS. A method for generating precise temporal patterns of retinal spiking using prosthetic stimulation. *J Neurophysiol* 95: 970–978, 2006.

Fried SI, Lasker ACW, Desai NJ, Eddington DK, Rizzo JF 3rd. Axonal sodium channel bands shape the response to electric stimulation in retinal ganglion cells. *J Neurophysiol* 101: 1972–1987, 2009.

Friedman DS, O'Colmain BJ, Muñoz B, Tomany SC, McCarty C, de Jong PTVM, Nemesure B, Mitchell P, Kempen J, and Eye Diseases Prevalence Research Group. Prevalence of age-related macular degeneration in the United States. *Arch Ophthalmol* 122: 564–572, 2004.

Fujikado T, Morimoto T, Kanda H, Kusaka S, Nakauchi K, Ozawa M, Matsushita K, Sakaguchi H, Ikuno Y, Kamei M, Tano Y. Evaluation of phosphenes elicited by extraocular stimulation in normals and by suprachoroidal-transretinal stimulation in patients with retinitis pigmentosa. *Graefes Arch Clin Exp Ophthalmol* 245: 1411–1419, 2007.

Gekeler F, Messias A, Ottinger M, Bartz-Schmidt KU, Zrenner E. Phosphenes electrically evoked with DTL electrodes: a study in patients with retinitis pigmentosa, glaucoma, and homonymous visual field loss and normal subjects. *Invest Ophthalmol Vis Sci* 47: 4966–4974, 2006.

Gerding H, Eckmiller RE, Hornig R, Ortmann V, Kolck A, Taneri S. Safety assessment and acute clinical tests of epiretinal retina implants. *Invest Ophthalmol Vis Sci* 43: E-Abstract 4488, 2002.

Hu EH, Dacheux RF, Bloomfield SA. A flattened retina-eyecup preparation suitable for electrophysiological studies of neurons visualized with trans-scleral infrared illumination. *J Neurosci Methods* 103: 209–216, 2000.

Humayun MS, de Juan E Jr, Weiland JD, Dagnelie G, Katona S, Greenberg R, Suzuki S. Pattern electrical stimulation of the human retina. *Vision Res* 39: 2569–2576, 1999.

Humayun MS, Weiland JD, Fujii GY, Greenberg R, Williamson R, Little J, Mech B, Cimmarusti V, Boemel GV, Dagnelie G, de Juan E Jr. Visual perception in a blind subject with a chronic microelectronic retinal prosthesis. *Vision Res* 43: 2573–2581, 2003.

Jensen RJ, Rizzo JF 3rd. Thresholds for activation of rabbit retinal ganglion cells with a subretinal electrode. *Exp Eye Res* 83: 367–373, 2006.

Jensen RJ, Rizzo JF 3rd. Responses of ganglion cells to repetitive electrical stimulation of the retina. *J Neural Eng* 4: 1–6, 2007.

Jensen RJ, Rizzo JF 3rd. Activation of retinal ganglion cells in wild-type and *rd1* mice through electrical stimulation of the retinal neural network. *Vision Res* 48: 1562–1568, 2008.

Klaver CCW, Wolfs RCW, Vingerling JR, Hofman A, de Jong PTVM. Age-specific prevalence and causes of blindness and visual impairment in an older population. *Arch Ophthalmol* 116: 653–658, 1998.

Li L, Hayashida Y, Yagi T. Temporal properties of retinal ganglion cell responses to local transretinal current stimuli in the frog retina. *Vision Res* 45: 263–273, 2005.

Marc RE, Jones BW, Watt CB, Strettoi E. Neural remodeling in retinal degeneration. *Prog Retin Eye Res* 22: 607–655, 2003.

Margalit E, Thoreson WB. Inner retinal mechanisms engaged by retinal electrical stimulation. *Invest Ophthalmol Vis Sci* 47: 2606–2612, 2006.

O'Brien BJ, Isayama T, Richardson R, Berson DM. Intrinsic physiological properties of cat retinal ganglion cells. *J Physiol* 538: 787–802, 2002.

O'Hearn TM, Sadda SR, Weiland JD, Maia M, Margalit E, Humayun MS. Electrical stimulation in normal and retinal degeneration (*rd1*) isolated mouse retina. *Vision Res* 46: 3198–3204, 2006.

Rizzo JF 3rd, Jensen RJ, Loewenstein J, Wyatt J. Unexpectedly small percepts evoked by epiretinal electrical stimulation in blind humans. *Invest Ophthalmol Vis Sci* 44: E-Abstract 4207, 2003.

Rizzo JF 3rd, Wyatt J, Loewenstein J, Kelly S, Shire D. Methods and perceptual thresholds for short-term electrical stimulation of human retina with microelectrode arrays. *Invest Ophthalmol Vis Sci* 44: 5355–5361, 2003.

Robblee LS, Lefko JL, Brummer SB. Activated Ir: an electrode suitable for reversible charge injection in saline solution. *J Electrochem Soc* 130: 731–733, 1983.

Rose TL, Robblee LS. Electrical stimulation with Pt electrodes. VIII. Electrochemically safe charge injection limits with 0.2 ms pulses. *IEEE Trans Biomed Eng* 37: 1118–1120, 1990.

Roska B, Werblin FS. Vertical interactions across ten parallel, stacked representations in the mammalian retina. *Nature* 410: 583–587, 2001.

Sekirnjak C, Hottowy P, Sher A, Dabrowski W, Litke AM, Chichilnisky EJ. Electrical stimulation of mammalian retinal ganglion cells with multielectrode arrays. *J Neurophysiol* 95: 3311–3327, 2006.

Sekirnjak C, Hottowy P, Sher A, Dabrowski W, Litke AM, Chichilnisky EJ. High-resolution electrical stimulation of primate retina for epiretinal implant design. *J Neurosci* 28: 4446–4456, 2008.

Shyu J-S, Maia M, Weiland JD, O'Hearn T, Chen S-J, Margalit E, Suzuki S, Humayun MS. Electrical stimulation in isolated rabbit retina. *IEEE Trans Neural Syst Rehabil Eng* 14: 290–298, 2006.

Stett E, Barth W, Weiss S, Haemmerle H, Zrenner E. Electrical multisite stimulation of the isolated chicken retina. *Vision Res* 40: 1785–1795, 2000.

Vaney D. A quantitative comparison between the ganglion cell populations and axonal outflows of the visual streak and periphery of the rabbit retina. *J Comp Neurol* 189: 215–233, 1980.

Völker M, Shinoda K, Sachs H, Gmeiner H, Schwarz T, Kohler K, Inhoffen W, Bartz-Schmidt KU, Zrenner E, Gekeler F. In vivo assessment of subretinally implanted microphotodiode arrays in cats by optical coherence tomography and fluorescein angiography. *Graefe's Arch Clin Exp Ophthalmol* 242: 792–799, 2004.

Wong YT, Chen SC, Seo JM, Morley JW, Lovell NH, Suaning GJ. Focal activation of the feline retina via a suprachoroidal electrode array. *Vision Res* 49: 825–833, 2009.

Zhou JA, Woo SJ, Park SI, Kim ET, Seo JM, Chung H, Kim SJ. A suprachoroidal electrical retinal stimulator design for long-term animal experiments and in vivo assessment of its feasibility and biocompatibility in rabbits. *J Biomed Biotechnol* 2008: Article 547428 (1–10), 2008.